

Chapter 4. Semiconductor Surface Studies

Academic and Research Staff

Professor John D. Joannopoulos, Dr. Arnaldo Dal Pino, Dr. Robert D. Meade

Graduate Students

Tomas A. Arias, Kyeongjae Cho, Andrew M. Rappe, Jing Wang

Technical and Support Staff

Imadiel Ariel

4.1 Introduction

Sponsor

Joint Services Electronics Program
Contract DAALO3-92-C-0001

Understanding the properties of surfaces of solids and the interactions of atoms and molecules with surfaces has been of extreme importance both from technological and academic points of view. The recent advent of ultrahigh vacuum technology has made possible microscopic studies of well-characterized surface systems. The way atoms move to reduce the energy of the surface, the number of layers of atoms involved in this reduction, the electronic and vibrational states that result from this movement, and the final symmetry of the surface layer are of utmost importance in arriving at a fundamental and microscopic understanding of the nature of clean surfaces, chemisorption processes, and the initial stages of interface formation.

The theoretical problems associated with these systems are quite complex. However, we are currently at the forefront of solving the properties of real surface systems. In particular, we are continuing our efforts in developing new techniques for calculating the total ground-state energy of a surface system from "first principles," so that we can provide accurate theoretical predictions of surface geometries and behavior. Our efforts in this program have concentrated in the areas of surface growth, surface reconstruction geometries, structural phase transitions, and chemisorption.

4.2 Surface Reconstruction

The (7x7) reconstruction of Si(111) is perhaps the most complex and widely studied surface of a solid. Since its discovery through low-energy electron diffraction (LEED) more than thirty years ago, an enormous amount of effort has been expended to elucidate the properties of this important surface. Based on this work, it is now generally accepted that the geometry of the (7x7) reconstruction is described by the dimer-atom-stacking-fault (DAS) model as proposed by Takayanagi et al. The complexity of this geometry, however, has defied any complete and realistic theoretical treatment of its properties. The only progress that could be made theoretically was by isolating and modeling bits and pieces of the surface. The only attempt at a complete work used an empirical tight-binding model to study the Si(111)-(7x7) reconstruction in a supercell geometry with 196 atoms.

In this work, we have exploited the power of the state of the art in parallel computation to demonstrate the feasibility of performing *ab initio* calculations with supercells approaching 1000 atoms. Specifically, we have performed the first *ab initio* calculation of the Si(111)-(7x7) using a supercell geometry with 700 effective atoms. These calculations predict the fully relaxed atomic geometry of this system, allow construction of theoretical scanning tunneling microscope (STM) images as a function of bias voltages, and predict the energy difference between the (7x7) and (2x1) reconstructions.

The DAS model for the Si(111)-(7x7) surface reconstruction is shown in figure 1. The unit-cell boundary is outlined by a dashed line. The largest solid circles denote the twelve atoms. The smaller solid circles denote six rest atoms that lie one layer below the surface and are threefold coordinated. There is also a single corner hole in each unit cell. Together, these 19 atoms account for the 19 unbonded electrons on the reconstructed surface.

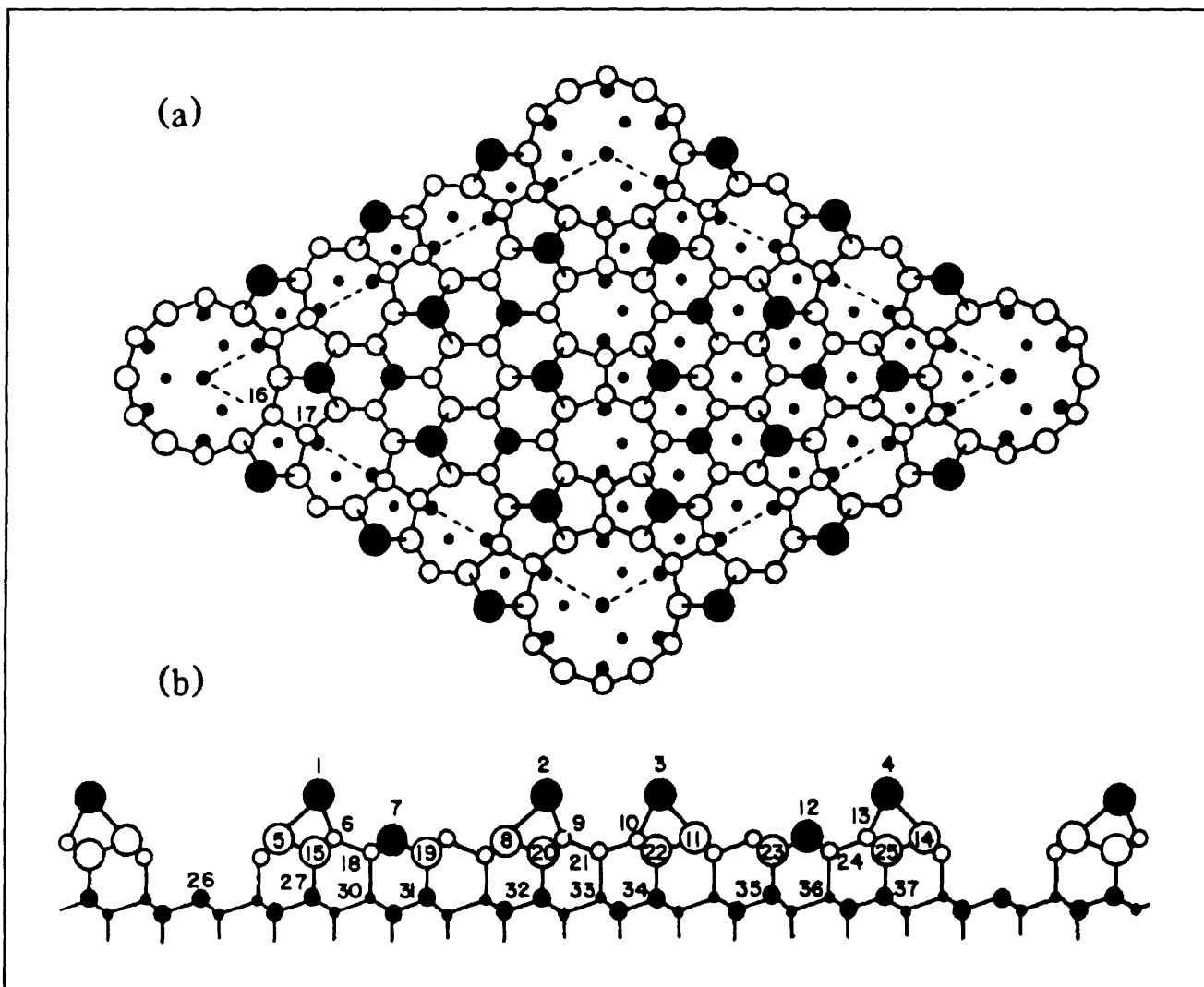


Figure 1. (a) Top view of the DAS model for the Si(111)-(7x7) surface reconstruction. The (7x7) unit cell is outlined. Atoms at increasing distances from the surface are indicated by circles of decreasing size. The large solid circles denote the twelve adatoms, the smaller solid circles represent the rest atoms. The faulted half of the unit cell is on the left. Small open circles denote the dimers, while small solid circles and dots represent atoms in the unreconstructed layers. (b) Side view. Atoms on the lattice plane along the long diagonal of the surface unit cell are shown with larger circles than those behind them. The numbers label the 37 unique atoms in the four-layer slab. All others are related by symmetry operations.

The smallest solid circles denote the fourth layer of atoms below the surface on the unfaulted half of the unit cell. Nine dimers are present two layers below the surface. One dimer is labeled by atoms with the number 16 and 17. The side view shows that the stacking sequence in the right half of the unit is the same as in bulk Si, while the stacking sequence in the left half is faulted.

Our model system consists of a supercell with a slab geometry containing vacuum on both sides. Periodic boundary conditions are applied in all directions. The slab contains the adatom layers and four surface layers shown in figure 1(b) plus a mirror image reflection in the vertical direction.

Thus, the supercell consists of eight layers of atoms with adatom layers on both slab surfaces and a region of 10 Å of vacuum. The 400 silicon atoms and the vacuum layer make this supercell equivalent to a 700-atom system. Unit-cell dimensions are 22 Å x 2 Å x 26 Å.

All atoms were allowed to move freely except the innermost layer, which was frozen in its bulk position. Thus, our model of the surface includes the relaxation of three surface layers in addition to the adatom layer. The atoms were assumed to be in their fully relaxed positions when the forces on the ions were converged to 0.15 eV/Å.

Table 1 shows the relaxed ionic positions. The computed positions in the surface plane are nearly identical with those from the tight-binding calculations. The most significant differences involve expansion of the surface layers away from the bulk layer. Compared to the tight-binding calculations, the adatoms move ~ 0.03 Å away from the bulk layer. The rest atoms move ~ 0.02 Å toward the bulk layer. Most of the remaining atoms move ~ 0.05 Å away from the bulk layer. However, atoms directly below adatoms move only ~ 0.03 Å,

	Atom	X	Y	Z
Adatoms	1	1.500	1.500	1.662
	2	4.492	4.491	1.594
	3	6.002	6.002	1.555
	4	9.005	9.005	1.603
First-layer atoms	5	1.033	1.033	-0.057
	6	1.958	0.993	-0.058
	7	2.481	2.481	0.348
	8	4.021	4.022	-0.155
	9	4.974	4.050	-0.099
	10	5.980	5.057	-0.135
	11	6.478	6.478	-0.163
	12	8.019	8.019	0.345
	13	9.029	8.059	-0.104
	14	9.472	9.472	-0.111
Second-layer atoms	15	1.504	1.504	-1.512
	16	1.162	0.006	-1.057
	17	1.800	0.007	-1.042
	18	2.492	1.499	-0.867
	19	2.969	2.969	-0.863
	20	4.494	4.495	-1.561
	21	5.403	4.780	-1.046
	22	6.004	6.004	-1.567
	23	7.532	7.532	-0.871
	24	8.505	7.510	-0.874
	25	8.998	8.998	-1.537
Third-layer atoms	26	0.001	0.001	-3.986
	27	1.500	1.500	-4.416
	28	1.006	-0.002	-3.989
	29	1.990	0.000	-3.964
	30	2.499	1.499	-3.946
	31	2.997	2.997	-3.951
	32	4.499	4.499	-4.460
	33	5.496	4.512	-3.973
	34	5.999	5.999	-4.440
	35	7.497	7.497	-3.933
	36	8.505	7.496	-3.930
	37	9.001	9.001	-4.414

Table 1. Relaxed atomic positions for the adatom layer and the first three surface layers for the *ab initio* (7x7) calculation. The coordinate system is the same as in reference 10. All reduced coordinates (X, Y, Z) are with respect to the Cartesian system indicated in figure 1, where the x axis is along the cubic [110] direction, and the y axis is along the [111] direction outward normal to the surface. The actual atomic coordinates (x, y, z) are related to (X, Y, Z) by the scaling relations $x = aX$, $y = aY/\sqrt{3}$, $z = aZ/\sqrt{24}$, where $a=3.85$ Å is the (1x1) surface hexagonal lattice constant.

resulting in a more distorted adatom configuration. The atoms two layers directly below move the most compared to the tight-binding calculations, relaxing ~ 0.10 Å away from the bulk layer. The relative heights of adatoms 1, 2, 3, and 4 are 0.085, 0.031, 0.000, and 0.038 Å, respectively. Experimental LEED values are 0.120, 0.080, 0.0, and 0.040.

Having generated the electronic wave functions in our pseudopotential calculation, we proceeded to make theoretical STM figures. In figure 2, we compare the theoretical results (top) with corresponding experiments at a tip voltage of 2 V (bottom) for both occupied and unoccupied states.

The theoretical STM probe was placed 3.8 Å above the surface adatom layer. The probe height is limited by the presence of a second surface layer above the probe due to the periodic replication of the unit cell. The theoretical grey scale was matched to the experimental grey scale at the tops of the adatoms and bottoms of the corner holes, and linearly interpolated in between. Experiments show a variation of 2-3 Å corresponding to this scale. The corresponding theoretical variation is 5 Å. Depths greater than 3 Å are set to minimum intensity in order to match the experimental grey scale.

The most fundamentally interesting part of this calculation is the comparison of formation energies of the (7x7) reconstruction and the (2x1) surface. Cleavage of Si to create the (111) surface results in a (2x1) metastable structure. This surface must then be annealed to generate the stable (7x7) structure. We find that the (7x7) reconstruction is energetically favorable over the metastable (2x1) surface by 60 meV per (141) cell. Our absolute values are 1.179 eV for the (7x7) surface and 1.239 eV for the (2x1).

The calculations discussed in this section were made possible because of the considerable computational power associated with massively parallel architectures. The calculations elevate *ab initio* investigations to a new echelon and demonstrate that studies of complex material systems with supercells containing nearly an order of magnitude more atoms than previously possible are now feasible.

4.3 Computation at Large Length Scales

As we discussed in the previous section, with recent advances in highly parallel computer architecture, calculations on systems with hundreds of atoms are now tractable. This not only permits more comfortable extraction of the thermodynamic

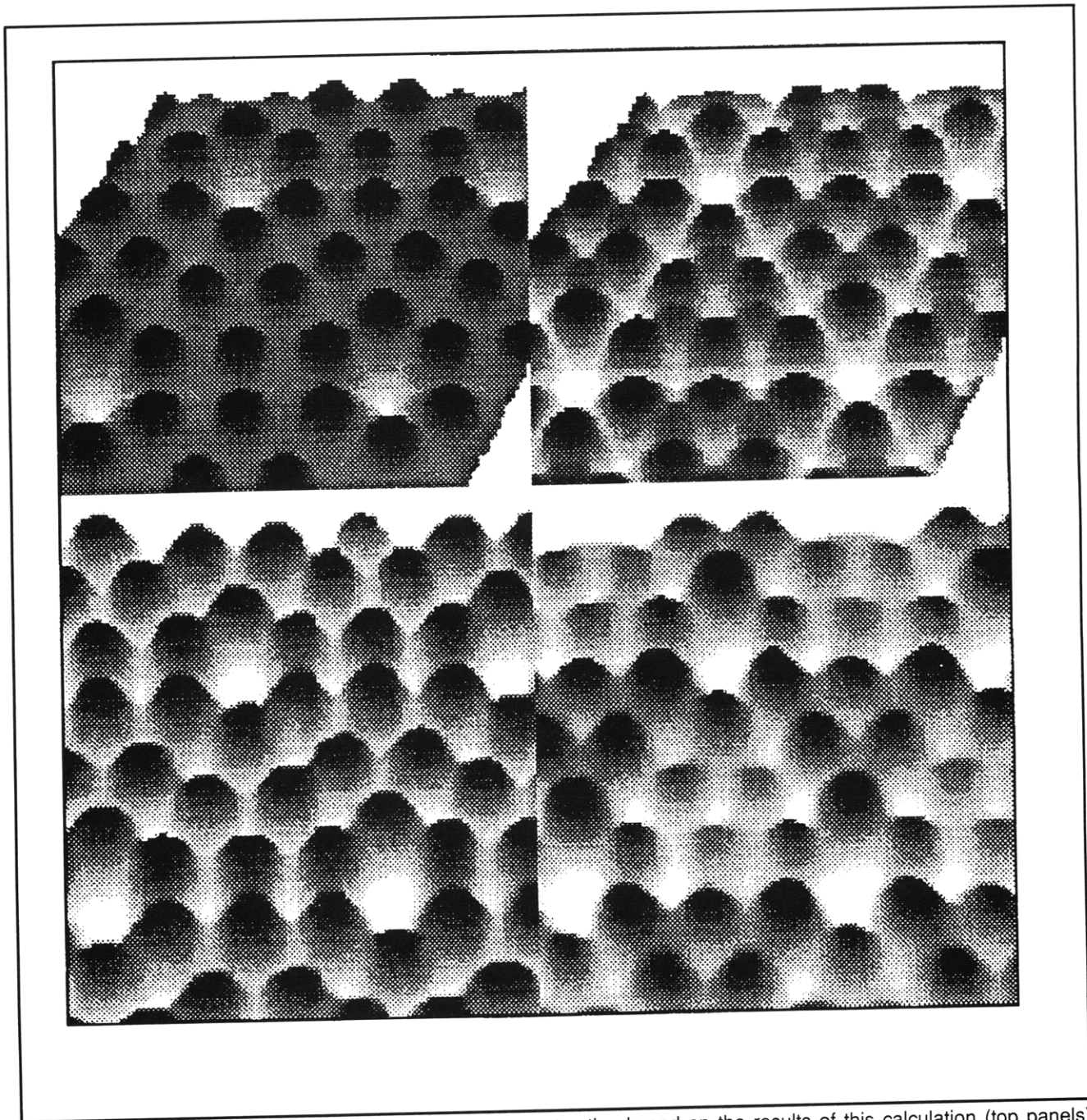


Figure 2. STM images of the Si(111)-(7x7) surface reconstruction based on the results of this calculation (top panels) and the experimental results of Avouris and Wolkow (bottom panels). Shown are unoccupied (left panel) and occupied (right panel) state contributions. The determination of the grey scale in the top panels is described in the text.

limit but also extends the qualitative level of complexity in accessible problems. However, with growing interest in calculations involving larger systems, it has been demonstrated that as the longest physical length scale in a calculation increases, integration of the fictitious electronic equations of motion becomes dominated by fluctuations in the electronic Hartree energy ("charge sloshing"). These fluctuations force the time step

for integration of the equations of motion to approach zero as the system size increases. While the onset of this instability depends on the physics of the system under study, the effect has been demonstrated dramatically in a silicon system of six primitive cells (~ 46 Å long) at 8 Ry. To fully benefit from the next generation of computer technologies, an approach free of charge sloshing is needed.

Recently, conjugate-gradient procedures introduced by Teter, Payne, Allan, and Gillan for relaxing the electronic wave functions at fixed atomic arrangements have been shown not to exhibit the aforementioned instability and to consume an order of magnitude less CPU time than the best fictitious electronic dynamics schemes. Despite this improvement, performing a dynamics calculation with conjugate-gradient techniques is very costly because of the tight tolerances to which the electronic problem must be solved (typically $10 \mu\text{V}/\text{atom}$) to yield stable atomic trajectories.

Very recently we have overcome these difficulties and introduced a new technique for performing finite-temperature *ab initio* total-energy calculations at long length scales. The method involves the introduction of a new class of energy functionals and an efficient scheme for performing iterative solutions.

To demonstrate the practicality of the new technique for long-length-scale systems, we have performed tests using a system that is well over 50 \AA long. In particular, we have determined the phonon spectrum of Si through the velocity-velocity autocorrelation function of the ions in our calculation. After projecting the ionic displacements from our calculation onto the allowed k states and the known purely longitudinal and transverse polarization vectors, we then determine the frequencies present in the time of autocorrelation functions of these spatial *Fourier coefficients* with the maximum entropy method. Taking the frequencies of the peak values of the resulting spectra, we compare our parameter-free results with the experimentally measured phonon frequencies in figure 3 and find excellent agreement. Our spectra clearly and accurately reproduce not only the celebrated flattening of the lower acoustic (TA) modes as one moves away from the Γ point but also the delicate splitting of the optic modes along Δ . Note that the calculation also accurately reproduces the lowest frequency acoustic mode despite its period of nearly 1 ps and manifests the delicate splitting of the optic modes, which beat against each other with even longer periods. This illustrates that our dynamics technique produces reliable ionic trajectories even over periods of picoseconds and is thus very precise.

4.4 Publications

Arias, T., M. Payne, and J.D. Joannopoulos. "Ab-Initio Molecular Dynamics at Large Length-Scales." *Phys. Rev. B* 45: 1538 (1992).

Arias, T., M. Payne, and J.D. Joannopoulos, "Ab-Initio Molecular Dynamics: Analytically Con-

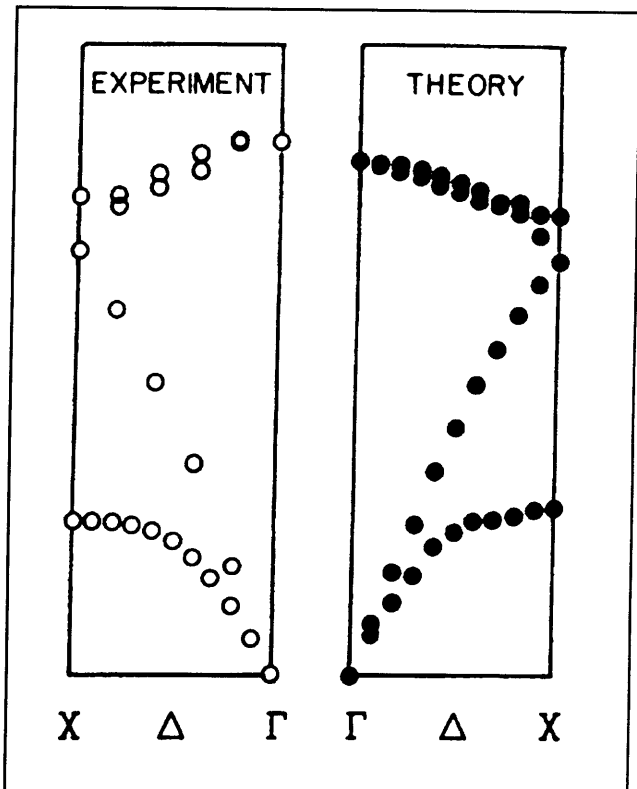


Figure 3. Phonon spectrum as determined from maximum peak values of MEM fits. These values are completely *ab initio* with no free parameters. The left-hand panel displays experimental data (13, 14) and the right hand panel displays frequencies from our dynamically determined trajectories.

tinued Energy Functionals and Insights into Iterative Solutions." *Phys. Rev. Lett.* 69: 1077 (1992).

Brommer, K., B. Larson, M. Needels, and J.D. Joannopoulos. "Implementation of the Car-Parrinello Algorithm for Ab-Initio Total Energy Calculations on a Massively Parallel Computer." In *Computers in Physics*.

Brommer, K., M. Needels, B. Larson, and J.D. Joannopoulos. "Ab-Initio Theory of the S:(III) (7x7) Surface Reconstruction - A Challenge for Massively Parallel Computation." *Phys. Rev. Lett.* 68: 1355 (1992).

Kaxiras, E., O. Alerhand, J. Wang, and J.D. Joannopoulos. "Theoretical Modelling of Heteroepitaxial Growth Initiation." *Mat. Sci. Eng. B* 14: 245 (1992).

Payne, M., G. Francis, M. Needels, E. Tarnow, P. Dallot, P. Bristowe, and J.D. Joannopoulos. "Ab-Initio Investigations of Surfaces and Grain Boundaries in Germanium." In *Ordering at Sur-*

faces and Interfaces. New York: Springer Verlag, 1992, p. 169.

Rappe, A., A. Dal Pino, M. Needels, and J.D. Joannopoulos. "Mixed Basis Pseudopotential Method for Iterative Diagonalization Techniques." *Phys. Rev. B* 46: 7353 (1992).

Rappe, A., J.D. Joannopoulos, and P. Bash. "A Test of the Utility of Planewaves for the Study of Molecules from First Principles." *J. Am. Chem. Soc.* 114: 6466 (1992).